ence of Si-Si bonding in the hydridopolycarbosilane is difficult to confirm by ^{29}Si NMR spectroscopy, as the Si-Si regions overlap with Si-H regions.

The formation of Si-Si bonding in the reduced polymer (with loss of hydrogen) after isolation, but prior to the sample analysis, could account for the low hydrogen content by elemental analysis. Samples of the reduced polymer have been observed to gradually increase in viscosity, eventually becoming rubbery and insoluble, and develop pressure when stored in sealed containers exposed to light. This is consistent with cross-linking through Si-Si bond formation and hydrogen loss.

The ethyl groups, as expected, are not affected by the reduction and remain in the hydridopolycarbosilane. Residual Grignard end groups in the chloropolycarbosilane, if any, would be converted to a magnesium aluminum hydride complex during the reduction.[23] Subsequent aqueous acid workup would result in the corresponding hydrocarbon end group, as shown in reactions 5 and 6.

$$\geq SiCH_2MgCl + LiAlH_4/Et_2O \rightarrow \geq SiCH_2MgAlH_4 + LiCl \quad (5)$$

$$\geq SiCH_2MgAlH_4 \xrightarrow{\text{excess } HCl/H_2O} \geq SiMe + MgCl_2 + H_2 + Al^{3+} + Cl^- \quad (6)$$

Part III: Hydridopolycarbosilane (from Nonaqueous Workup). The polymeric products from the nonaqueous workup are tacky, yellow solids which, unlike those prepared by aqueous workup, rapidly develop a whitish coating on exposure to air. The IR spectrum of this polymer is similar to that from the aqueous workup, except for two additional peaks at 1930 and 670 cm^{-1}. These peaks, in addition to elemental analysis showing 6.64% aluminum, suggest that residual Al-H_x functionality is present.[24] $LiAlH_4$ itself is insoluble in the pentane used to extract the polymer from the residue and therefore not likely to be a contaminant. Furthermore, the polymer had a transparent yellow color with no sign of suspended solid.[25]

The ^1H NMR spectrum of this polymer contains a broad, complex peak between -0.6 and +1.5 ppm, on which is superimposed a narrower peak between 0.8 and 1.1 ppm. The Si-H peaks are similar to those of the polymer derived from the aqueous workup, appearing at 3.6-3.9, 3.9-4.1, and 4.1-4.3 ppm. Their integration ratio with respect to the Si-CH_2Si protons is considerably below the approximately 1:1 ratio seen for the polymer derived from the aqueous workup. Difficulty in separating byproducts of $LiAlH_4$ reductions of polymeric halosilanes by nonaqueous methods has been previously observed.[16a]

Acknowledgment. We thank Dr. Todd Trout and Dr. Corrina Czekaj for helpful discussions and assistance during the course of this work. This work was supported by grants from the Air Force Office of Scientific Research (AFOSR-89-0439) and a DARPA/ONR (URI Program on High-Temperature Advanced Structural Composites).

(23) Gaylord, N. G. *Reduction With Complex Metal Hydrides*; Interscience: New York, 1956; p 70.

(24) These peaks are observed when the IR spectrum of $LiAlH_4$ was run in Nujol.

(25) The possibility of a colloidal suspension of the $LiAlH_4$ in the polymer cannot be excluded.

Structure and Bonding in the Unsymmetrically Hydrido-Bridged Heterobimetallic Complex $(\eta^5\text{-}C_5H_5)_2Mo(\mu\text{-}H)(\mu\text{-}CO)Co(CO)_3$

Jing-Cherng Tsai, Ralph A. Wheeler,* Masood A. Khan, and Kenneth M. Nicholas*

Department of Chemistry and Biochemistry, University of Oklahoma, Norman, Oklahoma 73019

Received August 28, 1990

Long-term reaction of $Cp_2Mo(\eta^2\text{-}CO_2)$ (Cp = $\eta^5\text{-}C_5H_5$) with $HCo(CO)_4$ produces the novel hydride-bridged heterobimetallic complex $Cp_2Mo(\mu\text{-}H)(\mu\text{-}CO)Co(CO)_3$ (1) whose X-ray structure and bonding are described in detail. Complex 1 features a deficient electron count, a rare "reverse" unsymmetrical hydride bridge placing the hydride closer to the larger Mo atom [1.64 (3) Å vs 1.88 (3) Å to Co], and a close Mo-Co contact (2.8449 (4) Å). Analysis of 1 using extended Hückel calculations reveals that the metals bond to the hydride and carbonyl bridges in a four-center, four-electron bond. Despite the relatively short Mo-Co distance in 1, there is only a weak metal-metal bonding interaction.

Introduction

Molecules containing an early and a late transition metal in close proximity are being actively studied to search for new catalytic behavior derived from bifunctional activation of substrates[1] and, more fundamentally, to enhance our understanding of the varying bonding and reactivity features of different transition-metal centers. Already, these "early-late heterobimetallics" have shown the ability to incorporate hydrogen,[2] to bind CO in novel ways,[2] and thus to promise a rich reduction chemistry for CO[3] and potentially for CO_2.[4,5]

As part of our studies of the chemistry of coordinated carbon dioxide, we recently reported on the reactions of

* Address general correspondence to these authors.

(1) (a) Bruce, M. I. J. *J. Organomet. Chem.* **1985**, *283*, 339. (b) Bruce, M. I. *J. Organomet. Chem.* **1983**, *242*, 147. (c) Roberts, D. A.; Geoffroy, G. L. In *Comphrehensive Organometallic Chemistry*; Wilkinson, G., Stone, F. G. A., Abel, E. W., Eds.; Pergamon: Oxford, England, 1982; Vol. 6, Chapter 40.

(2) Stephan, D. W. *Coord. Chem. Rev.* **1989**, *95*, 41.

(3) Prominent reactions of CO include the Fischer-Tropsch process, the hydroformylation reaction, and the reduction of CO to methanol: (a) Anderson, R. B. *The Fischer-Tropsch Synthesis*; Academic Press: Orlando, FL, 1987. (b) Sheldon, R. A. *Chemicals from Synthesis Gas, Catalytic Reactions of CO and H_2*; D. Reidel: Dordrecht, The Netherlands 1983. (c) Falbe, J., Ed. *New Syntheses with Carbon Monoxide*; Springer-Verlag: Berlin, 1980.

0276-7333/91/2310-1344$02.50/0

$Cp_2Mo(\eta^2\text{-}CO_2)$ (Cp = $\eta^5\text{-}C_5H_5$) with a number of transition-metal hydride complexes, including $HCo(CO)_4$.[6] Long-term reaction of the latter species was found to produce the novel heterobimetallic compound $Cp_2Mo(\mu\text{-}H)(\mu\text{-}CO)Co(CO)_3$ (1) whose structure has been established with high precision by X-ray diffraction. The structural and bonding features of this complex are unusual in several respects including: (1) 1 possesses both a hydride and a carbonyl bridge; (2) the bridging hydride resides significantly closer (1.64 (3) Å) to the larger Mo atom than to the smaller Co atom (1.88 (3) Å); (3) the Mo–Co distance is a rather short 2.8449 (4) Å, but it has only a weak metal–metal bonding interaction. We will say more about metal–metal and metal–bridge bonding later, based on extended Hückel[7] molecular orbital calculations.

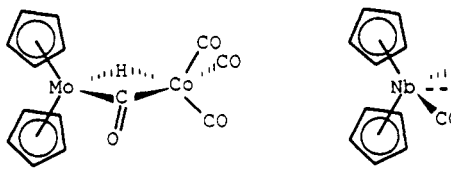

1

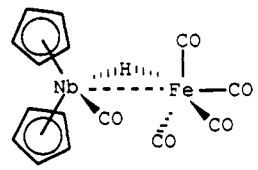

2

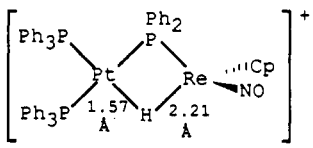

3

Although specific comparisons of the structural features of 1 with other bridged heterobimetallics will be presented in the Results and Discussion, we note at the outset that relatively few precisely located bridged hydrides have been characterized by X-ray or neutron diffraction. Among these, most are homodinuclear and (within experiment error) symmetrically bridged.[8] Furthermore, while unsymmetrically bridged hydrides have been noted for heterobimetallic complexes,[9] these with apparently only one exception[10] (vide infra) prior to our discovery of 1 show the hydride closer to the smaller metal center.

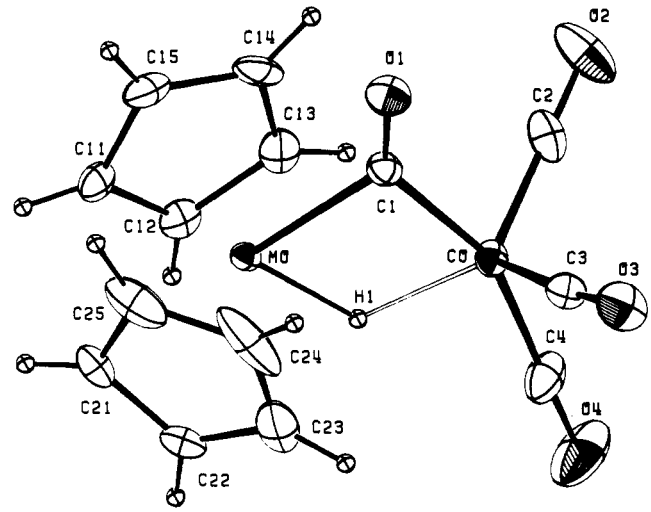

Figure 1. ORTEP drawing of $Cp_2Mo(\mu\text{-}H)(\mu\text{-}CO)Co(CO)_3$.

Table I. Selected Bond Lengths and Angles for $Cp_2Mo(\mu\text{-}H)(\mu\text{-}CO)Co(CO)_3$ (1)

(a) Bond Lengths (Å)			
Mo–Co	2.8449 (4)	Co–C(3)	1.772 (3)
Mo–C(1)	2.190 (2)	Co–C(4)	1.818 (3)
Mo–Cp(1)	1.969 (2)	Co–H(1)	1.88 (3)
Mo–Cp(2)	1.966 (3)	O(1)–C(1)	1.181 (3)
Mo–H(1)	1.64 (3)	O(2)–C(2)	1.146 (4)
Co–C(1)	1.905 (2)	O(3)–C(3)	1.144 (3)
Co–C(2)	1.768 (3)	O(4)–C(4)	1.135 (4)
(b) Bond Angles (deg)			
Cp(1)–Mo–Cp(2)	141.5 (1)	C(2)–Co–H(1)	114 (1)
Cp(1)–Mo–C(1)	104.4 (1)	C(3)–Co–C(4)	97.9 (1)
Cp(1)–Mo–H(1)	105 (1)	C(3)–Co–H(1)	133 (1)
Cp(2)–Mo–C(1)	105.4 (1)	C(4)–Co–H(1)	76 (1)
Cp(2)–Mo–H(1)	103 (1)	Mo–C(1)–Co	87.7 (1)
C(1)–Mo–H(1)	81 (1)	Mo–C(1)–O(1)	135.4 (2)
C(1)–Co–C(2)	92.0 (1)	Co–C(1)–O(1)	136.9 (2)
C(1)–Co–C(3)	89.7 (1)	Co–C(2)–O(2)	175.9 (2)
C(1)–Co–C(4)	158.0 (1)	Co–C(3)–O(3)	174.3 (2)
C(1)–Co–H(1)	83 (1)	Co–C(4)–O(4)	177.8 (3)
C(2)–Co–C(3)	113.0 (1)	Mo–H(1)–Co	108 (1)
C(2)–Co–C(4)	103.7 (1)		

We describe in detail herein the structure of 1 as well as its bonding features, particularly the bonding between the metal atoms and between the metals and the bridging ligands as revealed by extended Hückel calculations. These will be compared with structures of some related hydrido- and carbonyl-bridged heterobimetallics in order to place the molecule in the larger context of bridged heterobinuclear complexes.

Results and Discussion

Structure of $Cp_2Mo(\mu\text{-}H)(\mu\text{-}CO)Co(CO)_3$. The ORTEP diagram of $Cp_2Mo(\mu\text{-}H)(\mu\text{-}CO)Co(CO)_3$ is given in Figure 1 and a partial listing of bond lengths and angles is provided in Table I.

The structure is seen to consist of $(\eta^5\text{-}C_5H_5)_2Mo$– and –$Co(CO)_3$ fragments bridged by a hydride and by a carbonyl ligand. The three terminal CO ligands, along with the carbonyl and hydride bridges, form a distorted trigonal bipyramid around cobalt. The Co, C(2), C(3), and H(1) atoms lie in the pseudoequatorial plane (maximum deviation = 0.044 (2) Å for the Co atom); C(4)O(4) and the bridging carbonyl C(1)O(1) occupy the pseudoaxial positions within an "apical" angle of 158.0 (1)°. The molyb-

(4) (a) Behr, A. *Carbon Dioxide Activation by Metal Complexes*; VCH: Weinheim, Germany, 1988. (b) Darensbourg, D.; Kudaroski, R. A. *Adv. Organomet. Chem.* **1983**, *22*, 129. (c) Sneeden, R. P. A. In *Comprehensive Organometallic Chemistry*; Wilkinson, G., Stone, F. G. A., Abel, E. W., Eds.; Pergamon: Oxford, England, 1982; Vol. 8, Chapter 50.4. (d) Ito, T.; Yamamoto, A. In *Organic and Bioorganic Chemistry of Carbon Dioxide*; Inoue, S., Yamazaki, N., Eds.; Halstead Press: New York, 1982; Chapter 3, pp 79–151.

(5) Reactions of *coordinated* CO_2 are relatively limited: (a) Gambarotta, S.; Arena, F.; Floriani, C.; Zanazzi, P. F. *J. Am. Chem. Soc.* **1982**, *104*, 5082. (b) Aresta, M.; Quaranta, E.; Tomassi, I. *J. Chem. Soc., Chem. Commun.* **1988**, *450*. (c) Belmore, K. A.; Vanderpool, R. A.; Tsai, J.-C.; Khan, M. A.; Nicholas, K. M. *J. Am. Chem. Soc.* **1988**, *110*, 2004. (d) Tsai, J.-C.; Khan, M. A.; Nicholas, K. M. *Organometallics* **1989**, *8*, 2967.

(6) Tsai, J.-C.; Khan, M. A.; Nicholas, K. M. *Organometallics* **1991**, *10*, 29.

(7) (a) Wolfsberg, M.; Helmholz, L. *J. Chem. Phys.* **1952**, *20*, 837. (b) Hoffmann, R.; Lipscomb, W. N. *J. Chem. Phys.* **1962**, *36*, 2179. (c) Jordan, T.; Smith, H. W.; Lohr, L. L., Jr.; Lipscomb, W. N. *J. Am. Chem. Soc.* **1963**, *85*, 846. (d) Ammeter, J. H.; Bürgi, H.-B.; Thibeault, J. C.; Hoffmann, R. *J. Am. Chem. Soc.* **1978**, *100*, 3686.

(8) Reviews: (a) *Transition Metal Hydrides*; Bau, R., Ed., ACS Symposium Series 167; American Chemical Society: Washington, DC, 1978. (b) Teller, R. G.; Bau, R. *Struct. Bonding* **1981**, *44*, 1. (c) E.g. "A-frame" complexes: Sutherland, B. R.; Cowie, M. *Can. J. Chem.* **1986**, *64*, 464 and references therein.

(9) (a) Herrmann, W. A.; Biersack, H.; Balbach, B.; Wülknitz, P.; Ziegler, M. L. *Chem. Ber.* **1984**, *117*, 79. (b) Balbach, B. Baral, S.; Biersack, H.; Herrmann, W. A.; Labinger, J. A.; Scheidt, W. R.; Timmers, F. J.; Ziegler, M. L. *Oganometallics* **1988**, *7*, 325 and references therein. (c) Herrmann, W. A.; Biersack, H.; Balbach, B.; Ziegler, M. L. *Chem. Ber.* **1984**, *117*, 95. (d) Bau, R.; Kirtley, S. W.; Sorrell, T. N.; Winarko, S. *J. Am. Chem. Soc.* **1974**, *96*, 988. (e) Wong, K. S.; Scheidt, W. R.; Labinger, J. A. *Inorg. Chem.* **1979**, *18*, 136. (f) Skripkin, Y. V.; Pasynskii, A. A.; Kalimnikov, V. T.; Porai-Koshits, M. A.; Minacheva, L. K.; Antysyshkina, A. S. Ostrikova, V. N. *J. Organomet. Chem.* **1982**, *231*, 205.

(10) Powell, J.; Sawyer, J. F.; Stainer, M. V. R. *J. Chem. Soc., Chem. Commun.* **1985**, 1314.

denum coordination by the centroids of the Cp rings and the two bridging ligands is a distorted tetrahedron, with the (Cp centroid)–Mo–(Cp centroid) angle of 141° typical of Cp_2MoX_2 complexes.[11]

The most interesting features of the structure of 1 are located in the Mo(μ-H)(μ-CO)Co unit. The metal atoms are separated by 2.8449 (4) Å, a distance just slightly longer than the sum of the covalent radii (1.45 Å (Mo) + 1.26 Å (Co) = 2.71 Å)[12] and, in the range (2.7–2.9 Å) reported for other complexes assigned Mo–Co single bonds.[13] Most striking is the distinctly unsymmetrical hydride bridge having a distance to the larger Mo atom of 1.64 (3) Å and a longer distance of 1.88 (3) Å to the smaller Co for which we suggest the general term "reverse unsymmetrical" bridge. While the absolute values of M–H bond distances are recognized to be slightly underestimated (ca. 0.1 Å) by X-ray diffraction,[14] the high precision of the present structure determination leaves no doubt as to the relative position of the hydride closer to the Mo center. Of the few precisely determined Mo–H distances available for comparison, the Mo–H distance in 1 is similar to those found in terminal hydrides—e.g. 1.68 Å (neutron) in Cp_2MoH_2[15] and 1.76 (8) Å (X-ray) in $[Cp_2Mo(CO)H][CpMo(CO)_3]$[16]—and marginally shorter than the few reported bridging hydrides to Mo—1.7–1.9 Å.[17] On the other hand the Co–H distance in 1 is distinctly longer than previously recorded terminal distances—e.g. 1.41–1.67 Å for a series of 5-coordinate L_4Co–H complexes (X-ray and neutron)[18]—and marginally longer than the few reported bridging Co-H's—1.6–1.80 Å.[19] For the bridging carbonyl, the Co to carbonyl distance is 1.905 (2) Å, whereas the Mo–(μ-CO) distance is longer (as expected), 2.190 (2) Å. Both of these values are unexceptional for a normal μ_2-carbonyl bridging Co (1.85–1.95 Å[20]) and Mo (2.00–2.27 Å[21]). The Co–C(1)–O(1) and Mo–C(1)–O(1) angles of 136.9 (2) and 135.4 (2)° further indicate no significant asymmetry or tendency toward semibridging in the bridging carbonyl of 1. Interestingly, this apparently "normal" bridging carbonyl represents something of an exception rather than the rule since a survey of structures containing bridging carbonyls to Mo in the Cambridge crystallographic data base revealed a majority with significantly unsymmetrical (i.e. semi and asymmetric) bridging.

Table II. Selected Structural Parameters for Early–Late Heterobimetallics of the Type $Cp_2ML(\mu\text{-H})M'L_n$[a]

$M'L_n$	M–H, Å	M′–H, Å	M–M′, Å	ref
$CpV(CO)_3$	1.96 (16)	1.66 (18)	3.713 (4)	9a
$Cr(CO)_5$	1.82 (10)	1.88 (10)	3.453 (2)	9b
$CpMn(CO)_2$	1.98 (8)	1.56 (8)	3.330 (2)	9c
$Mn_2(CO)_9$	1.91 (3) [M = Ta]	1.77 (5)	3.441 (1)	9b
$Fe(CO)_4$	1.91 (3)	1.61 (3)	3.324 (1)	9e
$Ni(CO)_3$	1.83	1.68	3.218	9f
$Co(CO)_4$	1.64 (3) [M = Mo]	1.88 (3)	2.8449 (4)	this work

[a] For all molecules except the last, ML = NbCO; for the last molecule, ML = Mo.

It is instructive to compare the structure of 1 with a series of compounds of the type $Cp_2(CO)Nb(\mu\text{-H})M'L_n$ wherein the $Cp_2(CO)NbH$ unit contacts the $M'L_n$ fragment through a hydride bridge, at a distance greater than 3 Å between metals.[9] 2 is a typical example, $Cp_2(CO)Nb(\mu\text{-H})Fe(CO)_4$, reported by Labinger's group.[9e] Unlike $Cp_2Mo(\mu\text{-H})(\mu\text{-CO})Co(CO)_3$, $Cp_2(CO)Nb(\mu\text{-H})Fe(CO)_4$ has neither a bridging carbonyl nor a short metal–metal distance. Instead, $Cp_2(CO)Nb(\mu\text{-H})Fe(CO)_4$ has a terminal CO attached to niobium and a long metal–metal contact of 3.32 Å. Furthermore, the Nb–H distance of 1.91 Å is longer than the Fe–H separation (1.61 Å). Other hydrido-bridged heterobimetallics with similar structures are listed in Table II, along with their relevant structural features. Note that in all cases the H–Nb distance is longer than the H–M′ distance, as expected simply on the basis of atomic size. Nonetheless, Herrmann and Labinger[9b] have suggested that on the basis of covalent radii the hydride in these complexes resides closer to the Nb center than expected for a "symmetric" Nb–H–M′ bonding picture. Clearly, the effect, if significant, is modest compared to that observed in 1 where the hydride resides closer to the larger Mo atom. Bonding between the metals and the bridging hydride for the compounds in Table II is typically described as three-center, two-electron bonding arising by electron donation from the Nb–H bond to the electron-deficient $M'L_n$ fragment.

We find the most dramatic prior example of "reverse unsymmetrical" hydride bridging to be represented in the Re–Pt complex 3 in which the H–M distance to the Re atom is some 0.6 Å shorter than to the Pt center.[10] This complex has an electron count of 32 and can be formulated as having an 18-electron $Cp(NO)(\mu\text{-}PPh_2)Re^{I}$–H unit serving as a two-electron donor to the electron deficient 14-electron $(Ph_3P)_2Pt^{II}(\mu\text{-}PPh_2)$ unit. Further comment on the analogy between 3 and 1 is deferred to the bonding section.

Chemical Bonding in $Cp_2Mo(\mu\text{-H})(\mu\text{-CO})Co(CO)_3$. Several different qualitative descriptions of bonding between Mo- and Co-centered fragments arise from various possible ways to count electrons in $Cp_2Mo(\mu\text{-H})(\mu\text{-CO})Co(CO)_3$. One possible method of electron counting begins by partitioning the bridging ligands to give Cp_2MoH and $Co(CO)_4$ fragments. Assigning each Cp and each hydride ligand a 1– formal charge makes the d^6 Mo atom formally Mo^{3+}, d^3. The Cp^- ligands each donate six electrons to Mo, whereas H^- contributes two, so that Cp_2MoH has 2 (Mo^{3+}, d^2) + 2 × 6 (2Cp^-) + 2 (H^-) = 17 electrons. Similarly, Co(0) is d^9 and $Co(CO)_4$ has 9 (Co(0)) + 4 × 2 (4CO) = 17 electrons. Although both Mo and Co could satisfy the 18-electron rule by forming a metal–metal bond, this description would neglect the interaction between Mo and the bridging carbonyl and between Co and the bridging hydride ligand.

An alternative bonding description that emphasizes the roles of the bridging ligands, rather than metal–metal in-

(11) See, e.g.: (a) Crotty, D. E.; Anderson, T. J.; Glick, M. D.; Oliver, J. P. *Inorg. Chem.* **1977**, *16*, 2346. (b) Forder, R. A.; Gale, G. D.; Prout, K. *Acta Crystallogr.* **1975**, B31, 297. (c) Calderon, J. L.; Cotton, F. A.; Legzdins, P. *J. Am. Chem. Soc.*, **1969**, *91*, 2528. (d) Kutoglu, A. *Kristallogr.* **1971**, *132*, 437.

(12) Porterfield, W. W., *Inorganic Chemistry*, Addison-Wesley: Reading, MA 1984; p 168.

(13) (a) Schmid, G.; Bartl, K.; Boese, R. *Z. Naturforsch.* **1977** 32B, 1277. (b) Beurich, H.; Vahrenkamp, H. *Angew. Chem., Int. Ed. Engl.* **1981**, *20*, 98. (c) Salzer, A.; Egolf, T.; Linowsky, L.; Petter, W. *J. Organomet. Chem.* **1981**, *221*, 339.

(14) Coppens, P.; Sabine, T. M.; Delaplane, R. G.; Ibers, J. A. *Acta Crystallogr.* **1969**, *B25*, 2451.

(15) Schultz, A. J.; Stearley, K. L.; Williams, J. M.; Mink, R.; Stucky, G. D. *Inorg. Chem.* **1977**, *16*, 3303.

(16) Adams, M. A.; Folting, K.; Huffman, J. C.; Caulton, K. G. *Inorg. Chem.* **1979**, *18*, 3020.

(17) For representative examples see: (a) Petersen, J. L.; Dahl, L. F.; Williams, J. M. *J. Am. Chem. Soc.* **1974**, *96*, 6610. (b) King, R. B.; Fu, W.-K.; Holt, E. M. *Inorg. Chem.* **1986**, *25*, 2390. (c) Horton, A. D.; Mays, M. J.; Raithby, P. R. *J. Chem. Soc.*, Dalton *Trans.* **1987**, 1557.

(18) Whitfield, J. M.; Watkins, S. F.; Tupper, G. B.; Baddley, W. H. *J. Chem. Soc., Dalton Trans.* **1977**, *407* and references therein.

(19) (a) Roland, E.; Vahrenkamp, H. *Organometallics* **1983**, *2*, 183. (b) Pursianinen, J.; Pakkanen, T. A. *J. Organomet. Chem.* **1986**, *309*, 187.

(20) See, e.g.: (a) Elder, M.; Hutcheon, W. L. *J. Chem. Soc. Dalton Trans.* **1972**, 175. (b) Leonowics, M. E.; Maydonovitch, D. J. *J. Am. Chem. Soc.* **1980**, *102*, 5101.

(21) See, e.g.: (a) Chisolm, M. H.; Kelly, R. L.; Cotton, F. A.; Extine, M. W. *J. Am. Chem. Soc.* **1978**, *100*, 2256. (b) Gibson, C. P.; Dahl, L. F. *Organometallics* **1988**, *7*, 543.

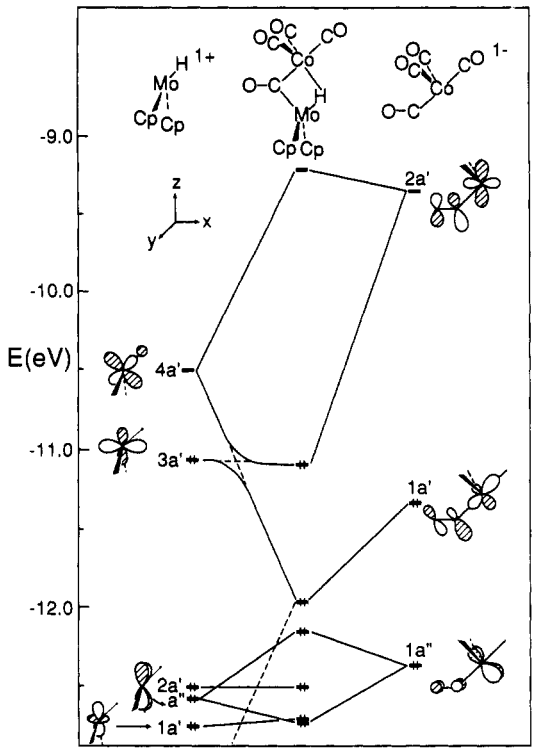

Figure 2. Interaction of Cp_2MoH^+ and $Co(CO)_4^-$ fragments in the geometry indicated at the top producing the molecular orbitals of $Cp_2Mo(\mu\text{-}H)(\mu\text{-}CO)Co(CO)_3$, shown in the center of the figure.

teraction, is provided by the isolobal analogy.[22] Specifically, since d^4 Cp_2Mo is isolobal with CH_2, Cp_2MoH is isolobal with methyl radical, and the $Cp_2Mo(\mu\text{-}H)(\mu\text{-}CO)Co(CO)_3$ molecule is comparable to an acyl complex of Co. The 16-electron complex $Co(CO)_3(COR)$[23] (R = CH_3 or Cp_2MoH) attempts to satisfy the 18-electron rule at cobalt by engaging in an agostic interaction (a three-center two-electron bond)[24] with the neighboring C–H or Mo–H bond.

Neither the isolobal analogy nor the simple electron-counting procedure described above gives a completely adequate description of metal–metal and metal–bridge bonding. Electron counting neglects the metal interaction with bridging ligands, whereas the isolobal analogy leads to an agostic picture of Mo–H interaction with Co that neglects the effects of the carbonyl bridge on metal–hydride bonding. The inadequacy of these simple models, as well as the unusual position of the bridging hydride nearer to the early transition metal, impelled us to characterize the bonding between metals and bridging ligands in $Cp_2Mo(\mu\text{-}H)(\mu\text{-}CO)Co(CO)_3$ by extended Hückel molecular orbital calculations. In the process, we found an interesting description of metal–metal and metal–hydride bonding, enforced by the presence of the bridging carbonyl ligand.

To characterize bonding within the planar core of $Cp_2Mo(\mu\text{-}H)(\mu\text{-}CO)Co(CO)_3$ we examined the orbital interactions important in forming the molecule from separate Cp_2MoH^+ and $Co(CO)_4^-$ fragments. The left side of Figure 2 displays the orbitals of Cp_2MoH^+, the right side of the figure shows the orbitals of $Co(CO)_4^-$ fragment, and the orbitals of the composite molecule—Cp_2Mo $(\mu\text{-}H)(\mu\text{-}CO)Co(CO)_3$—appear in the middle of Figure 2. The energy levels in Figure 2 are labeled according to their symmetry with respect to the mirror plane containing the Mo, Co, μ-H, and μ-CO atoms. Further computational details are reported in the Experimental Section.

Although the Cp_2MoH^+ molecule is unknown, its frontier orbitals are easily envisioned in terms of the carbenoid orbitals of the Cp_2M fragment first calculated by Brintzinger and others in the 1970's.[25] The LUMO of Cp_2MoH^+ is labeled 4a′ in Figure 2 and is concentrated in the Mo xz level—a π orbital in the plane bisecting the (Cp centroid)–Mo–(Cp centroid) angle. 4a′ is thus analogous to the π orbital of methylene but modified by its σ-antibonding character between the Mo xz and hydride s orbitals. The Cp_2MoH^+ HOMO contains a mixture of Mo z^2 with $x^2 - y^2$ and represents one analogue of the methylene σ level. The resulting orbital has $z^2 - x^2$ character—the shape of $x^2 - y^2$, but oriented in the xz plane. Immediately below the HOMO of $Cp_2Mo(\mu\text{-}H)(\mu\text{-}CO)Co(CO)_3$ is a level labeled 2a′ that is not drawn out. This orbital is primarily Mo–Cp bonding and will not participate in metal–bridge bonding in any major way. Just below 2a′ is the a″ level consisting primarily of Mo yz and the 1a′ level concentrated on the Cp rings, but containing a small contribution from Mo z^2.

The orbitals of the $Co(CO)_4^-$ fragment—drawn on the right of Figure 2—are similar to those of the generic C_{2v} ML_4 fragment.[26] In a local coordinate system with the x axis parallel to the (μ-CO)–Co bond and z perpendicular to x, in the plane of the figure, and containing Co, the LUMO of $Co(Co)_4^-$ (labeled 2a′) has a large contribution from Co xz. The Co component of 2a′ interacts in an antibonding way with the bridging carbonyl's π^* orbital and differs from the corresponding orbital of the C_{2v} ML_4 fragment mainly by having an admixture of carbon p_x and s. The carbon p_x and s orbitals mix with carbon z upon bending the CO ligand and serve to hybridize the carbon component of 2a′ toward the eventual position of Mo. The HOMO of $Co(CO)_4^-$ (1a′) resembles the metal-centered, σ level of an idealized C_{2v} ML_4 fragment and contains $z^2 - x^2$ as well as some Co p_x character. The bonding interaction between Co and carbon p_x is reduced by carbon s and p_z mixing, a mixing that hybridizes the p_x away from Co and reorients it toward the Cp_2MoH^+ fragment. The carbon p and s contributions give 1a′ substantial carbon lone-pair character and make it a potential electron donor orbital toward the Cp_2MoH^+ fragment. Finally, the lowest energy orbital of $Co(CO)_4^-$ shown in Figure 2 is a″—the Co yz level, hybridized away from the equatorial carbonyls by added p_y character.

The interaction of the Cp_2MoH^+ and $Co(CO)_4^-$ fragments to form $Cp_2Mo(\mu\text{-}H)(\mu\text{-}CO)Co(CO)_3$ gives the energy

(22) (a) Halpern, J. *Homogeneous* Catalysis; Advances in Chemistry 70; American Chemical Society: Washington, DC, 1968; pp 1–24. (b) Mingos, D. M. P. *Nature (London), Phys. Sci.* **1972**, *236*, 99. (c) Elian, M.; Chen, M. M.-L.; Mingos, D. M. P.; Hoffmann, R. *Inorg. Chem.* **1976**, *15*, 1148. (d) Wade, K. *Adv. Inorg. Chem. Radiochem.* **1976**, *18*, 1. (e) For a summary, see: Hoffmann, R. *Angew. Chem.* **1982**, *94*, 725; *Angew. Chem., Int. Ed. Engl.* **1982**, *21*, 711.

(23) Although its structure is unknown, experimental evidence exists for $Co(CO)_3(COR)$ as an intermediate in the hydroformylation reaction: (a) Collman, J. P.; Hegedus, L. S.; Norton, J. R.; Finke, R. G. *Principles and Applications of Organotransition Metal Chemistry*; University Science Books: Mill Valley, CA, 1987; pp 624–625 and references therein. (b) Heck, R. F. *J. Am. Chem. Soc.* **1963**, *85*, 651.

(24) Agostic interactions are usually considered as three-center, two-electron bonds involving H: (a) Brookhart, M.; Green, M. L. H.; Wong, L.-L. *Prog. Inorg. Chem.* **1988**, *36*, 1. (b) LaPlaca, S. J.; Ibers, J. A. *Inorg. Chem.* **1965**, *4*, 778. (c) Bailey, N. A.; Jenkins, J. M.; Mason, R.; Shaw, B. L. *J. Chem. Soc., Chem. Commun.* **1965**, 237.

(25) (a) Brintzinger, H. H.; Bartell, L. S. *J. Am. Chem. Soc.* **1970**, *92*, 1105. (b) Lauher, J. W.; Hoffmann, R. *J. Am. Chem. Soc.* **1976**, *98*, 1729.

(26) (a) Burdett, J. K. *J. Chem. Soc., Faraday Trans. 2* **1974**, *70*, 1599. (b) Elian, M.; Hoffmann, R. *Inorg. Chem.* **1975**, *14*, 1058. (c) Albright, T. A. *Tetrahedron* **1982**, *38*, 1339. (d) Albright, T. A.; Burdett, J. K.; Whangbo, M.-H. *Orbital Interactions in Chemistry*; Wiley-Interscience: New York, 1985; p 358ff.

levels shown in the center of Figure 2. Clearly, the strongest, most stabilizing interaction between the two fragments is the mixing between the Cp_2MoH^+ LUMO (4a′) and the HOMO of $Co(CO)_4^-$. Both orbitals are directed for large, mutual overlap and their moderate difference in energies ensures a strong interaction. A second orbital located on the Cp_2MoH^+ fragment also mixes with 4a′ to cancel its hydride contribution to the final MO. This second orbital has Mo–H σ-bonding character, and its effect is represented by the dashed line starting from the lower left side of Figure 2. The resulting orbital, 4, is

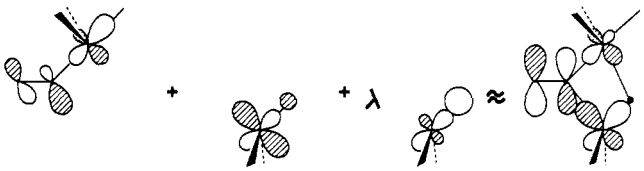

4

strongly bonding between the bridging carbonyl and both metals but is weakly Mo–Co antibonding. It has only a tiny hydride contribution and is approximately nonbonding between hydride s and the metal orbitals.

Other interactions between Cp_2MoH^+ and $Co(CO)_4^-$ fragment orbitals are much weaker. Although the Cp_2MoH^+ HOMO and the LUMO of $Co(CO)_4^-$ have large overlap, their large energy difference prevents strong mixing. The resulting orbital—the HOMO of 1—has only weak bonding character between Mo and Co and between Mo and the bridging carbonyl. Similarly, Cp_2MoH^+ 2a′ interacts very little with $Co(CO)_4^-$ and remains essentially unchanged in energy. The fragment yz orbitals, labeled a″, interact strongly, but give a net repulsive interaction between the fragments, as both the bonding and antibonding combinations are occupied in $Cp_2Mo(\mu\text{-}H)(\mu\text{-}CO)Co(CO)_3$. Both the metal–metal σ and σ^* levels show up at low energy because of their bonding interactions with the ligands.

The qualitative picture of metal–metal and metal–bridge bonding that emerges from Figure 2 is therefore governed primarily by the strongest interaction shown, the interaction between Cp_2MoH^+ 4a′ and 1a′ of $Co(CO)_4^-$. The main consequence of this interaction is evident from a comparison of the metal–metal and metal–hydride bonding in $Cp_2Mo(\mu\text{-}H)(\mu\text{-}CO)Co(CO)_3$, represented in 5 with that

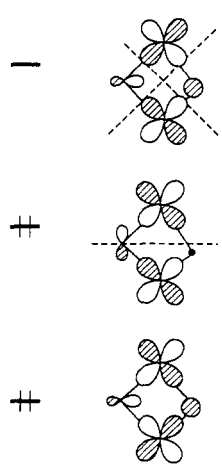

5

in the related $Cp_2(CO)Nb(\mu\text{-}H)M'L_n$ molecules. Strong Mo–H and Co–carbonyl bonding, somewhat weaker Co–H bonding, and a bonding Mo–Co interaction are concentrated primarily in one low-energy molecular orbital sketched at the bottom of 5. The filled orbital derived from the LUMO of Cp_2MoH^+ and the $Co(CO)_4^-$ HOMO appears in the center of 5. It has metal–hydride nonbonding character, but is bonding between each metal and the carbonyl bridge. This orbital, minus the carbonyl contribution, would be empty in $Cp_2(CO)Nb(\mu\text{-}H)M'L_n$ and would represent the nonbonding orbital of the three-center, two-electron bond between Nb, H, and M′. The primary difference in bonding among metals and bridging hydride is therefore the bonding carbonyl contribution to the central orbital drawn in 5, which keeps the orbital low enough in energy to be occupied in $Cp_2Mo(\mu\text{-}H)(\mu\text{-}Co)Co(CO)_3$. The result is a four-center, four-electron bond involving both metals and both bridging ligands.

Substituting a π-donor ligand such as Cl^- for the electron-accepting[27,28] CO bridge could potentially change this picture. With donor bridges, the nonbonding member resulting from the four-center interaction among the two metals and the bridges would have antibonding character between the metals and the donor bridge. A strong enough donor ligand in the bridging position could potentially push this level up high enough in energy to become unoccupied. For the experimentally known *cis*-$Cp(CO)(NO)Re(\mu\text{-}PCy_2)(\mu\text{-}H)Pt(PPh_3)_2^+$, the bridging phosphide is apparently not a strong enough donor, as this level remains occupied and the metal–hydride bonding is analogous to that described for $Cp_2Mo(\mu\text{-}H)(\mu\text{-}CO)Co(CO)_3$.

A variety of orbitals in addition to those sketched in 5 involve metal–metal interactions and render metal–metal bonding in $Cp_2Mo(\mu\text{-}H)(\mu\text{-}CO)Co(CO)_3$ extremely weak and almost nonexistent. Since the Mo–Co σ and σ^* orbitals (not shown in Figure 2) appear at low energy due to bonding interactions with ligand orbitals, they are filled and contribute nothing to Mo–Co bonding. Similarly, both the metal–metal π and π^* orbitals of a″ symmetry are filled. Within the plane of the metals and the bridging ligands, the occupied MO derived from 4a′ and 1a′ of $Co(CO)_4^-$ has Mo–Co π^* character and serves to weaken Mo–Co bonding. The major part of the weak Mo–Co bonding is thus carried by the HOMO of the $Cp_2Mo(\mu\text{-}H)(\mu\text{-}CO)Co(CO)_3$ molecule. Although this orbital has a small antibonding contribution from Mo *xz* and Co *xz*, the small, dative interaction between 3a′ and the CO p_z component of 2a′ more than compensates. Nonetheless, the single interaction between Mo 3a′ and Co 2a′ is not strong enough to merit assigning the $Cp_2Mo(\mu\text{-}H)(\mu\text{-}CO)Co(CO)_3$ molecule a metal–metal bond. Although we lack a molecule containing an unambiguous Mo–Co single bond for direct, quantitative comparison, the small, positive Mo–Co overlap population[29] of 0.034 confirms the picture of a weak, bonding interaction between metals in $Cp_2Mo(\mu\text{-}H)(\mu\text{-}CO)Co(CO)_3$.

Finally, we try to address the question of why the hydride prefers to sit closer to Mo than to Co. Part of the reason is cobalt's greater electronegativity, which places its d orbitals lower in energy than those of Mo. Cobalt's low-energy d orbitals insure that the occupied MO's of 1 will contain some Co–H antibonding character. These

(27) The acceptor character of the CO bridge was verified by noting charge flow to the C and O atoms of the CO bridge upon bending it toward Co, similar to that in the report: Jemmis, E. D.; Pinhas, A. R.; Hoffmann, R. *J. Am. Chem. Soc.* **1980**, *102*, 2576.

(28) The bridging carbonyl's acceptor character is consistent with the model proposed by Cotton and Troup: Cotton, F. A.; Troup, J. M. *J. Am. Chem. Soc.* **1974**, *96*, 1233. Cotton, F. A. *Prog. Inorg. Chem.* **1976**, *21*, 1.

(29) Overlap populations are a calculated measure of bond order. A large positive number implies a strong bond; a large negative overlap population indicates a strong antibonding interaction: Mulliken, R. S. *J. Chem. Phys.* **1955**, *23*, 1833, 1841, 2338, 2343.

Table III. Crystal Data for 1

formula	$C_{14}H_{11}O_4CoMo$	data collcn range, deg	$0 < 2\theta < 55$
mol wt	398.11		
temp, °C	−110	tot. no. of reflcns measd	3040 ($\pm h,k,l$)
syst	monoclinic		
space group	$P2_1/n$	no. of reflcns used $[I > 2\sigma(I)]$	2399
a, Å	21.958 (5)		
b, Å	7.625 (2)	R^a	0.020
c, Å	8.204 (2)	$R_w{}^b$	0.025
β, deg	98.16 (3)	GOF[c]	0.98
V, Å^3	1359.7	largest shift/esd, final cycle	0.1
Z	4		
density, g/cm^3	1.945	ρ_{max} in the final diff map, e/Å^3	0.32
μ, cm^{-1}	20.3		

[a] $R = \sum||F_o| - |Fc||/\sum|F_o|$. [b] $R_w = [\sum w(|F_o| - |F_c|)^2|/\sum wF_o^2]^{1/2}$. [c] GOF $= [\sum w|F_o| - |F_c|)^2/(m - n)]^{1/2}$.

Co–H antibonding levels move up in energy and thus raise the total energy of the structure when the hydride is shifted closer to Co, a feature that was confirmed by our calculations. We know, however, that this is not the entire story; otherwise, the $Cp_2CONb(\mu\text{-}H)Fe(CO)_4$ structure would show the hydride closer to Nb. Our calculations in fact indicate that the hydride should rest closer to Nb than to Fe in $Cp_2CONb(\mu\text{-}H)Fe(CO)_4$. We believe that the discrepancy between calculation and experiment may be due either to our failure to optimize geometries fully or to the extended Hückel method's well-known difficulties in reproducing experimental bond lengths.

Conclusions

The complex $Cp_2Mo(\mu\text{-}H)(\mu\text{-}CO)Co(CO)_3$ displays several interesting features including the following: (1) it is the product of metal–hydride-mediated reduction of coordinated CO_2; (2) it provides a rare example of a "reverse unsymmetrical" hydrido bridge—one wherein the bridging hydride resides significantly closer to the larger metal atom; (3) it shows a Mo–Co distance of 2.85 Å, without displaying a strong metal–metal-bonding interaction.

Compared to previously described heterobimetallics,[2,9] bonding in $Cp_2Mo(\mu\text{-}H)(\mu\text{-}CO)Co(CO)_3$ differs in two major ways. First, metal–hydride bonding in $Cp_2(CO)Nb(\mu\text{-}H)Fe(CO)_4$ involves three-center, two-electron bonding; in $Cp_2Mo(\mu\text{-}H)(\mu\text{-}CO)Co(CO)_3$, the metals bond to the bridging hydride and carbonyl ligands in a four-center, four-electron bond. The occupied MO derived from the Cp_2MoH^+ 4a′ level and $Co(CO)_4^-$ 1a′ (Figure 2) represents the metal–hydride nonbonding member of the set arising from a four-center, four-electron interaction between Mo, Co, CO, and hydride and is primarily responsible for the unusual metal–hydride bonding. It also carries most of the metal–carbonyl bonding and is largely responsible for the stability of $Cp_2Mo(\mu\text{-}H)(\mu\text{-}CO)Co(CO)_3$ relative to the two fragments considered. The second unique feature of bonding in $Cp_2Mo(\mu\text{-}H)(\mu\text{-}CO)Co(CO)_3$ appears in the interaction between metals: despite the relatively short Mo–Co distance in $Cp_2Mo(\mu\text{-}H)(\mu\text{-}CO)Co(CO)_3$, there is only a very weak metal–metal bonding interaction. A significant portion of the weak metal–metal bonding in $Cp_2Mo(\mu\text{-}H)(\mu\text{-}CO)Co(CO)_3$ can be traced to the Mo d_{z^2} and Co p_z character of the HOMO.

Experimental Section

X-ray Structure Determination of 1. Crystals of 1 were obtained by allowing a toluene/pentane solution of $Cp_2Mo(CO_2)$ and excess $HCo(CO)_4$ to stand for 2–3 days at −20 °C under CO_2. A suitable crystal (0.15 × 0.15 × 0.20 mm) was mounted under a flush of nitrogen, and X-ray data were collected on an Enraf-Nonius diffractometer, using monochromated Mo Kα radiation (λ = 0.71069 Å), by the methods standard in this laboratory.[30]

Table IV. Atomic Coordinates for $Cp_2Mo(\mu\text{-}H)(\mu\text{-}CO)Co(CO)_3$

atom	x	y	z	$10^{-3}U$, Å^2
		(a) Non-Hydrogen Atoms		
Mo	0.13957 (1)	0.41143 (3)	0.47638 (3)	
Co	0.09546 (1)	0.24910 (4)	0.17009 (4)	
O(1)	0.2173 (1)	0.3939 (2)	0.1834 (2)	
O(2)	0.0629 (1)	0.5129 (3)	−0.0840 (3)	
O(3)	0.1587 (1)	−0.0406 (3)	0.0345 (3)	
O(4)	−0.0204 (1)	0.0617 (4)	0.1970 (4)	
C(1)	0.1722 (1)	0.3613 (3)	0.2405 (3)	
C(2)	0.0740 (1)	0.4113 (4)	0.0189 (3)	
C(3)	0.1350 (1)	0.0703 (4)	0.0955 (3)	
C(4)	0.0247 (1)	0.1367 (4)	0.1877 (4)	
C(11)	0.1352 (1)	0.6679 (3)	0.6145 (3)	
C(12)	0.0743 (1)	0.6299 (3)	0.5379 (3)	
C(13)	0.0744 (1)	0.6375 (3)	0.3668 (4)	
C(14)	0.1346 (1)	0.6798 (3)	0.3365 (4)	
C(15)	0.1725 (1)	0.6965 (4)	0.4883 (4)	
C(21)	0.1786 (1)	0.3303 (4)	0.7380(3)	
C(22)	0.1302 (1)	0.2130 (4)	0.6813 (3)	
C(23)	0.1487 (2)	0.1190 (4)	0.5500 (4)	
C(24)	0.2079 (2)	0.1781 (5)	0.5254 (4)	
C(25)	0.2265 (1)	0.3108 (5)	0.6403 (4)	
		(b) Hydrogen Atoms		
H(1)	0.0789 (15)	0.3109 (46)	0.3816 (41)	43 (9)
H(11)	0.1484 (14)	0.6781 (41)	0.7237 (40)	27 (8)
H(12)	0.0424 (14)	0.6032 (38)	0.5895 (39)	26 (8)
H(13)	0.0429 (14)	0.6225 (38)	0.2848 (39)	26 (8)
H(14)	0.1472 (14)	0.6890 (41)	0.2324 (39)	27 (8)
H(15)	0.2122 (14)	0.7268 (37)	0.5051 (36)	21 (7)
H(21)	0.1792 (12)	0.3982 (37)	0.8247 (37)	10 (7)
H(22)	0.0958 (15)	0.1933 (45)	0.7301 (43)	39 (9)
H(23)	0.1259 (17)	0.0381 (53)	0.4894 (47)	53 (11)
H(24)	0.2262 (19)	0.1336 (57)	0.4543 (54)	64 (13)
H(25)	0.2615 (16)	0.3808 (44)	0.6498 (42)	38 (9)

Table V. Parameters Used in the Extended Hückel Calculations[33]

atom	orbital	H_{ii}, eV	ζ_1 (C_1)[a]	ζ_2 (C_2)[a]
Mo	5s	−8.77	1.96	
	5p	−5.60	1.90	
	4d	−11.06	4.54 (0.5899)	1.90 (0.5899)
Co	4s	−9.21	2.00	
	4p	−5.29	2.00	
	3d	−13.18	5.55 (0.5680)	2.10 (0.6060)
C	2s	−21.40	1.625	
	2p	−11.40	1.625	
O	2s	−32.30	2.275	
	2p	−14.80	2.275	
H	1s	−13.60	1.30	

[a] Exponents and coefficients in the double-ζ expansion of transition-metal d orbitals.

The data were corrected for Lorentz and polarization effects; no absorption correction was applied since absorption was judged to be negligible. A summary of experimental X-ray parameters is provided in Table III. The structure was solved by the heavy-atom method. Initial refinement of all non-hydrogen atoms with anisotropic thermal parameters gave R = 0.026. At this stage a difference Fourier map showed all H atoms with peak heights between 0.56–0.93 e Å^3; the hydride atom had a peak height of 0.67 e Å^3 but was not included in the refinement. A subsequent difference Fourier map showed on peak at 0.68 e Å^3 at the location of the hydride, while the next highest peak was at 0.34 e Å^3. All the hydrogen atoms were refined with an isotropic temperature factor; the temperature factor of the hydride was third highest among the H atoms but not unusual in value and refined properly to its final value. All calculations were carried out by using the SHELX-76 program.[31] The atomic scattering factors were taken

(30) Khan, M. A.; Taylor, R. W.; Lehn, J. M.; Dietrich, B. *Acta Crystallogr.* 1988, *C44*, 1928.
(31) SHELX-76. Program for Crystal Structure Determination, University of Cambridge, England, 1976.

from ref 32. Atomic coordinates are given in Table IV.

Molecular Orbital Calculations. Calculations were performed by using average, experimental bond lengths and bond angles in an idealized geometry. Idealizations included (1) maintaining a mirror plane containing the two metal atoms and the bridging ligands, (2) assuming equal C-C bond lengths of 1.41 Å, C-H bond lengths of 1.1 Å, and a regular pentagonal geometry for the Cp rings, and (3) assuming Co-C bond lengths for the apical carbonyls of 1.905 Å. For the hypothetical compound with hydride closer to Co, the Mo-Co-H bond angle was maintained at the experimental value as the Co-H distance was shortened. Parameters for the extended Hückel calculations with weighted H_{ij}'s[7] are taken from the literature[33] and are reported in Table V.

Acknowledgment. K.M.N. is grateful for support provided by the Division of Chemical Sciences, Office of Basic Energy Sciences, U.S. Department of Energy (Grant 89ER 13997). R.A.W. thanks the Department of Chemistry and Biochemistry, University of Oklahoma, for supporting this work, University Computing Services for making computer time available through the College of Arts and Sciences, and the University of Oklahoma Research Council for a Junior Faculty Summer Research Fellowship.

Supplementary Material Available: Tables of anisotropic thermal parameters and complete interatomic distances and angles (3 pages); a table of observed and calculated structure factors (10 pages). Ordering information is given on any current masthead page.

(32) *International Tables for X-ray Crystallography*; Kynoch Press: Birmingham, U.K. 1974; Vol. IV, pp 99, 149.
(33) (a) Summerville, R. H.; Hoffmann, R. *J. Am. Chem. Soc.* 1976, *98*, 7240. (b) Kubacek, P.; Hoffmann, R.; Havlas, Z. *Organometallics* 1982, *1*, 180.

Propylene Hydroformylation in Supercritical Carbon Dioxide†

J. W. Rathke,* R. J. Klingler,* and T. R. Krause

Chemical Technology Division, Argonne National Laboratory, Argonne, Illinois 60439

Received October 30, 1990

The cobalt carbonyl catalyzed hydroformylation of propylene and related equilibrium and dynamic processes were investigated by means of high-pressure NMR spectroscopy with supercritical carbon dioxide (d = 0.5 g/mL) used as the reaction medium to avoid gas/liquid mixing problems associated with conventional solvents. At 80 °C, the hydroformylation proceeds cleanly in CO_2, giving a somewhat improved yield of linear to branched butyraldehyde products, 88%, without use of stirring. The rate of propylene hydroformylation and in situ measurements of the steady-state concentrations of catalytic intermediates [RC(O)Co(CO)$_4$, HCo(CO)$_4$, and Co$_2$(CO)$_8$] were found to be comparable to values for other linear-terminal olefins in nonpolar liquid media. For the hydrogenation of Co$_2$(CO)$_8$ (to form HCo(CO)$_4$) at 80 °C in CO_2, the equilibrium constant, $Kp = 8.8 \times 10^{-4}$ M atm^{-1}, and the rate constants for the forward and reverse reactions (1.6×10^{-6} atm^{-1} s^{-1} and 1.8×10^{-3} M^{-1} s^{-1}, respectively) compared closely with values for liquid methylcyclohexane solutions. Potential dynamic processes involving Co$_2$(CO)$_8$, Co$_4$(CO)$_{12}$, or HCo(CO)$_4$ were explored at temperatures up to 205 °C at 338 atm by means of ^{59}Co, ^{13}C, and ^{1}H NMR spectroscopy. Due to the low viscosity of the supercritical medium, linewidths for the ^{59}Co nucleus were decreased by a factor of about 6 compared to values in normal liquids. An NMR pressure-probe design that uses an efficient toroid detector is also described.

I. Introduction

Although supercritical fluids have seldom been explored for this purpose, they have properties that could make them nearly ideal media for conducting homogeneous catalytic processes that involve the reactions of gases with soluble liquid or solid substrates. Since only one phase is present, gas-liquid mixing, which is often rate limiting in liquid solvents, is not problematic for supercritical fluids. In addition, reactive gas concentrations in supercritical media are typically much higher than achievable in normal liquids. For example, the concentration of H_2 at 25 °C and a partial pressure of 300 atm in supercritical CO_2 is 12 M, while in water and in n-heptane the hydrogen concentrations under these conditions are only 0.23[1] and 1.8 M,[2] respectively. Perhaps of greatest significance, catalyst and product separations that normally would be accomplished by energy intensive distillations might be more efficiently achieved in supercritical fluids. Due to the sharp changes in solubilities of dissolved species with density of the supercritical medium,[3] separations might be accomplished by facile pressure alterations to control fluid density, and, in turn, catalyst or product solubility. A variety of processes for separating problematic mixtures such as ethanol/water and others using supercritical fluids have been proposed.[4-7]

In this report we describe in situ high-pressure NMR experiments relevant to the oxo process, which judged from the gas-liquid mixing problems complicating some of the earlier research,[8] might be expected to benefit from the use of supercritical media. The experiments were designed to determine the effect of supercritical CO_2 on the linear to branched aldehyde product ratio (which is of considerable industrial significance and is known to be concen-

†This research was supported by the Division of Chemical Sciences, Office of Basic Energy Sciences, U.S. Department of Energy.

(1) Linke, W. F. *Solubilities*; American Chemical Society: Washington, DC, 1949; Vol. 1, p 1077.
(2) Ungvary, F. *J. Organometal. Chem.* 1972, *36*, 363-370.
(3) McHugh, M.; Krukonis, U. *Supercritical Fluid Extraction*; Butterworths: Stoneham, MA, 1986.
(4) Defillippi, R. P.; Vivian, E. U.S. Patent 4,349,415, Sept 14, 1982.
(5) Hagen, R.; Hartwig, J. U.S. Patent 4,492,808, Jan 8, 1985.
(6) Victor, J. G. U.S. Patent 4,508,928 April 2, 1985.
(7) Bhise, V. S.; Hoch, R. U.S. Patent 4,437,938; March 20, 1984.
(8) Pruett, R. L. In *Advances in Organometallic Chemistry*; Stone, F. G. A. and West, R., Eds.; Academic Press: New York, 1979; Vol. 17, pp 1-60.

0276-7333/91/2310-1350$02.50/0